**Membrane and Water Treatment,** *Vol. 17, No. 3 (2026) 223-238*
https://doi.org/10.12989/mwt.2026.17.3.223

Techno-Press

# Trajectory analysis and design optimization of a horizontal oil-water separator: Role of hydrodynamic and dimensional parameters

Melouka Bellil*[1,2], Menouer Bennaoum[2], Ali Bellil[3]

[1]*Faculty of Nature and Life Sciences, Mustapha Stambouli University of Mascara, 305 Mamounia Road, Mascara, Algeria*
[2]*Faculty of Sciences and Technology, Mustapha Stambouli University of Mascara, 305 Mamounia Road, Mascara, Algeria*
[3]*Department of Chemical Engineering, Faculty of Chemistry, University of Sciences and Technology of Oran-MB,El Mnaouar, 1505, Bir ElDjir, Oran, Algeria*

*(Received July 23, 2025, Revised April 11, 2026, Accepted April 16, 2026)*

**Abstract.** The treatment of oil-contaminated industrial wastewater remains a critical environmental and economic challenge. This study presents a comprehensive hydrodynamic analysis and design optimization of a horizontal oil-water separator, integrating an automated control system with a theoretical trajectory model for oil droplets. This study develops a mathematical model based on force balance (buoyancy versus drag) under laminar flow conditions to predict droplet trajectories as functions of key hydrodynamic and dimensional parameters: droplet radius, inlet velocity, separator diameter, mass flow rate, and Reynolds number. The model yields explicit expressions for terminal rise velocity, rise time, residence time, and minimum required separator length. Parametric analysis reveals that smaller droplets (50 μm) dictate design requirements: at an inlet velocity of 0.005 m/s, a separator of radius 1.0 m requires a minimum length of 4.55 m to achieve complete separation, corresponding to a residence time of approximately 15 minutes. A critical mass flow rate of 0.5 kg/s is identified, below which buoyancy dominates and above which horizontal advection compromises efficiency. To maintain laminar conditions ($Re < 2300$), inlet velocity must not exceed 0.015 m/s for a 1.0 m diameter separator. The theoretical length-to-diameter ratio for the design droplet is approximately 2.3; applying a safety factor of 1.5–2.0 yields practical ratios of 3.4–4.6, aligning with industry standards (3:1 to 5:1). Quantitative design guidelines are summarized, including recommendations for separator diameter (≥1.0 m), maximum inlet velocity (≤0.015 m/s), and separator compartment sizing.

**Keywords:** hydrodynamic modeling; oil-water separator; parametric study; trajectory analysis; wastewater

## 1. Introduction

The oil industry plays a significant role in ensuring global energy supply. However, oil extraction generates substantial volumes of wastewater containing petroleum components, which require effective treatment before discharge. Oil companies operate across diverse locations and perform various tasks, among which the treatment of oil-contaminated water is crucial. Environmental regulations concerning oil discharge in wastewater have become increasingly stringent worldwide, driving significant efforts to regulate pollution in most industrialized

*Corresponding author, Associate Professor, E-mail: melouka.bellil@univ-mascara.dz


http://www.techno-press.org/mwt/5
ISSN: 2005-8624 (Print), 2092-7037 (Online)

countries [1].

Horizontal oil-water separators, including those based on American Petroleum Institute (API) design standards, are widely employed in the petroleum, chemical, and other industries to separate oil and its derivatives from water [2]. While traditional methods such as grease traps and skimming tanks exhibit limited efficiency in removing oil and grease [3], newer approaches offer cleaner and safer alternatives [4]. Recent advances in surface wettability engineering have led to the development of specialized membranes with enhanced oil-water separation performance, demonstrating the potential of materials-based solutions [5]. Numerous studies have developed highly effective treatment methods and disposal management strategies for oil and grease wastes to mitigate their environmental impact [6-8]. The efficiency and sustainability of oil-water separation methods represent a form of technological progress essential for environmental protection.

Treatment approaches range from simple physical methods - such as gravity separation, skimmer tanks, API separators, and coalescers - to more advanced techniques including electrocoagulation, activated carbon adsorption, oxidation processes, and membrane filtration [9-11]. Advanced computational approaches, including hierarchical clustering algorithms, have been applied to analyze complex hydraulic forces in fluid handling systems, demonstrating the value of data-driven methods for understanding flow phenomena [12].

Wastewater treatment methods generally fall into three main categories: physical, chemical, and biological. Physical methods; including sedimentation, membrane filtration, and flotation, enable contaminant separation without chemical transformation [13, 14]. Demulsifiers - chemical additives that prevent emulsification or break existing emulsions - are commonly used to destabilize oil-water emulsions, promoting droplet coalescence and facilitating separation. Biological methods rely on microorganisms to degrade organic contaminants in systems such as trickling filters, lagoons, and membrane bioreactors [15-17].

Understanding the fundamental hydrodynamics of multiphase systems is essential for optimizing separation processes. Recently, numerical approaches have been widely used to investigate complex fluid flow behavior in various engineering systems [18, 19].

Despite the availability of advanced treatment technologies, there remains a need for practical, physically based design tools for conventional gravity separators, particularly in applications where complex simulation resources are limited. Most existing design guidelines for horizontal oil-water separators rely on empirical rules or simplified residence time calculations that do not explicitly account for the coupled effects of droplet size, inlet velocity, separator geometry, and flow regime on separation performance.

This study adopts a hydrodynamic trajectory model for horizontal oil-water separators [20], based on fundamental force balance between buoyancy and drag under laminar flow conditions. The model yields explicit analytical expressions for terminal rise velocity, rise time, residence time, and minimum required separator length as functions of key parameters: droplet radius, inlet velocity, separator diameter, mass flow rate, and Reynolds number. Parametric analyses quantify the sensitivity of separator dimensions to each parameter, identifying critical thresholds for maintaining efficient separation. The theoretical length-to-diameter ratio derived from the model is compared with industry standards. The quantitative design guidelines provide a rational basis for preliminary separator sizing, with clear recommendations for diameter, length, inlet velocity, and the main separation chamber dimensions. Limitations of the model including the neglect of coalescence, droplet size distributions, and non-ideal flow patterns are acknowledged, with more advanced multiphase modeling approaches identified as directions for future research.

## 2. System description and integrated control strategy

The proposed oil removal system is based on gravitational separation within a horizontal two-compartment separator, which could be enhanced by an automated control system. The separation efficiency, governed by the hydrodynamic principles modeled in Section 3, could be monitored and controlled in real-time via a conductivity-based feedback loop. The detailed design, programming, and validation of such an automated control system-including the three solenoid valves and their integration with the conductivity sensor-are identified as a direction for future work beyond the scope of the present hydrodynamic study.

### 2.1 Separator design and operating principle

The separator consists of two primary compartments, Fig. 1. The first compartment acts as a sludge trap, facilitating the sedimentation of dense solids. The second compartment is the main separation chamber, where oil droplets rise via buoyancy under controlled laminar flow conditions. A coalescing filter within this chamber promotes the aggregation of fine oil droplets, accelerating the separation process. The treated water exits from a lower outlet, while the separated oil is evacuated from an upper outlet.

### 2.2 Integration of control with separation dynamics

The core of the automation strategy is the relationship between the local oil concentration and the electrical conductivity of the fluid. As an insulator, the presence of a dispersed oil phase reduces the measured conductivity. Under optimal laminar flow, a stable, stratified profile develops, with an oil-rich layer forming at the top of the separation compartment.

The primary conductivity sensor $C_1$ is positioned within the oil outlet channel, Fig. 1. Its location is determined by the model's prediction for the arrival of the separated oil front under design flow conditions. When the oil concentration at $C_1$ exceeds a set threshold (indicating a sufficient oil layer has accumulated), the measured conductivity drops. This triggers the control logic to open the oil evacuation solenoid valve $V_2$. Conversely, the system can be designed to open the treated water valve $V_3$ upon detecting high conductivity (primarily water) at a corresponding sensor or after a timed delay following oil removal. This closed-loop control directly links the physical separation outcome, predicted by the hydrodynamic model, to the system's automated actions, ensuring efficient phase separation and discharge.

### 2.3 Automated control sequence

The operational sequence, managed by a central control unit (e.g., PLC or microcontroller), is as follows:

- Filling/Separation: Inlet valve $V_1$ is open. Valves $V_2$ (oil) and $V_3$ (water) are closed. The mixture enters, and separation occurs.
- Oil Discharge: Sensor $C_1$ in the oil outlet monitors conductivity. A signal below a threshold (high oil concentration) triggers the opening of $V_2$ to evacuate the separated oil layer.
- Water Discharge: Following oil removal, the system can initiate water discharge. This can be triggered by a secondary sensor, a conductivity recovery signal at $C_1$, or a pre-set settling time, leading to the opening of $V_3$.

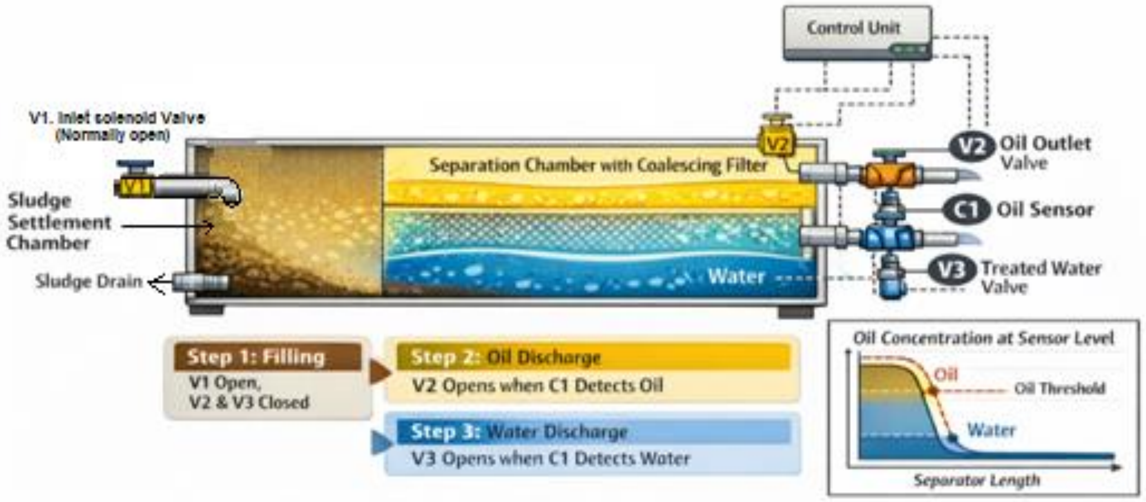


Figure 1. Schematic diagram of the automated horizontal oil-water separator with integrated monitoring and control system. The separator comprises a sludge settlement chamber followed by a separation chamber equipped with a coalescing filter. Solenoid valves V1 (inlet), V2 (oil outlet), and V3 (treated water outlet) are actuated based on signals from the conductivity sensor C1 located at the oil outlet. The control unit governs the sequential filling, oil discharge, and water discharge operations. The inset illustrates the simulated oil concentration profile along the separator length at the oil outlet elevation, supporting the sensor placement

This integrated approach ensures the separator operates autonomously, responding to the actual separation performance rather than a fixed timer, thereby optimizing efficiency and preventing cross-contamination of outlets.

## 3. Mathematical modeling of droplet trajectory and separation dynamics

### 3.1 Physical premises and simplifying assumptions

The modeling is based on a set of classical assumptions for studying gravitational separation under laminar flow conditions. The current model focuses on the primary separation of discrete, non-emulsified oil droplets:

- Oil droplet: It is assimilated to a rigid sphere of radius $r$, density $\rho_{oil}$ and dynamic viscosity $\eta$. Its shape remains spherical throughout its motion (no deformation).
- Flow: The wastewater flow is steady, uniform, and horizontal (with single horizontal velocity $v_x = v_0$). The flow regime is assumed to be laminar ($Re < 2300$), a necessary condition to avoid turbulence that would disperse the droplets.
- Free oil droplets: Only non-emulsified droplets are considered. Stable emulsions (submicron droplets) require coalescence mechanisms or chemical treatments, which fall outside the scope of this study.
- Dominant force: Archimedes' buoyancy force exceeds the droplet weight ($\rho_{oil} < \rho_w$) ensuring natural droplet rise.

### 3.2 Force balance in horizontal and vertical directions

The motion of an oil droplet within the wastewater flow is governed by four forces: Its weight P, Archimedes' buoyancy force $F_{ar}$, the horizontal driving force exerted by the flowing water $F_x$, and the fluid dynamic drag force (friction force) $F_r$ opposing the droplet's relative motion.

The net upward force results from the competition between buoyancy and weight:

$$F_y = F_{ar} - P = (\rho_w - \rho_{oil})V_{oil}g \tag{1}$$

where $\rho_w$ is the water density $\rho_{oil}$ and $V_{oil}$ are the density and volume of droplet oil respectively.

When viscous forces dominate over inertial forces, the drag force on a spherical droplet is given by Stokes' Law:

$$F_r = -6\pi\eta r v_r \tag{2}$$

where $v_r$ is the velocity of the droplet relative to the surrounding fluid, $\eta$ the dynamic viscosity and $r$ the droplet radius of oil.

Resolving forces in the horizontal and vertical directions and applying Newton's second law yields the equations of motion. For the horizontal direction, assuming constant horizontal velocity $v_x$, the driving force exactly balances the horizontal drag (Given by Stokes' Law):

$$F_x = F_r = 6\pi\eta r v_x \tag{3}$$

The vertical motion (with vertical velocity component $v_y$ is governed by:

$$-6\pi\eta r v_y + \rho_w V_{oil} g - \rho_{oil} V_{oil} g = \rho_{oil} V_{oil} \frac{dv_y}{dt} \tag{4}$$

where g is the gravitational acceleration. This simplifies to a first-order linear differential equation for the vertical velocity:

$$\frac{dv_y}{dt} + \frac{6\pi\eta r}{\rho_{oil} V_{oil}} v_y = \left(\frac{\rho_w}{\rho_{oil}} - 1\right) g \tag{5}$$

The resolution of the differential equation could take the following case, depending on the boundary conditions at the entrance to the separator:

$$y = \frac{b}{a} t + \frac{b}{a^2}(e^{-at} - 1) \tag{6}$$

where $a = \frac{6\pi\eta r}{\rho_{oil} V_{oil}}$ and $b = \left(\frac{\rho_w}{\rho_{oil}} - 1\right) g$. The vertical displacement as a function of horizontal distance (the droplet trajectory equation) is then provided as follows:

$$y = Ax + B(e^{-Cx} - 1) \tag{7}$$

With coefficients: $A = \frac{b}{a v_0}$, $B = \frac{b}{a^2}$ $and$ $C = \frac{a}{v_0}$.

### 3.3 Establishing Laminar Flow: Reynolds number and design constraints

To ensure unidirectional horizontal movement of water, the flow must be laminar. Laminar flow minimizes pressure losses and provides stability, allowing the flow field to be treated as steady with negligible spatial and temporal variations.

The nature of the flow is characterized by the Reynolds number $R_e$, a dimensionless parameter defined as:

$$R_e = \frac{vD}{\mu} = \frac{4Q_m}{\pi\rho_w\,\mu_w\,D} \tag{8}$$

where:

$D$ is the inlet characteristic diameter of the separator.
$v$ is the characteristic velocity.
$\mu_w$ is the kinematic viscosity of water.
$Q_m$ is the mass flow rate.
$\rho_w$ is the water density.

For pipe flow or separators with circular cross-section, a Reynolds number below 2300 indicates laminar flow. This condition must be satisfied to maintain a stable, predictable droplet trajectory. The laminar-flow condition ($R_e < 2300$) provides a practical criterion for selecting the minimum allowable diameter or maximum flow rate consistent with laminar regime requirements.

Furthermore, the resistance to flow in a pipe due to viscous shear is quantified by a dimensionless parameter $f$ given by $f = 64/R_e$ for fully developed laminar flow in a circular cross-section. This inverse proportionality means that as flow becomes slower or more viscous, the friction factor $f$ increases. This highlights the strong dependence of frictional forces on the Reynolds number and justifies the assumption of laminar flow for accurate prediction of droplet trajectories.

### 3.4 Rise time, residence time and separation condition

The terminal rise velocity $u_t$ of an oil droplet in water, derived from the force balance (buoyancy = drag) under Stokes' regime, is given by:

$$u_t = \frac{2}{9}\frac{r^2 g}{\eta_w}(\rho_w - \rho_{oil}) \tag{9}$$

The corresponding rise time to reach the top of a separator of radius $R$ is given by:

$$t_{rise} = \frac{R}{u_t} = \frac{9R\eta_w}{2r^2 g(\rho_w - \rho_{oil})} \tag{10}$$

The residence time available in the separator of length L is given by:

$$t_{res} = \frac{L}{v_0} \tag{11}$$

For complete separation, the droplet must reach the top before exiting the separator ($t_{res} > t_{rise}$), which yields to the minimum required separator length:

$$L_{min} = v_0\frac{9R\eta_w}{2r^2 g(\rho_w - \rho_{oil})} \tag{12}$$

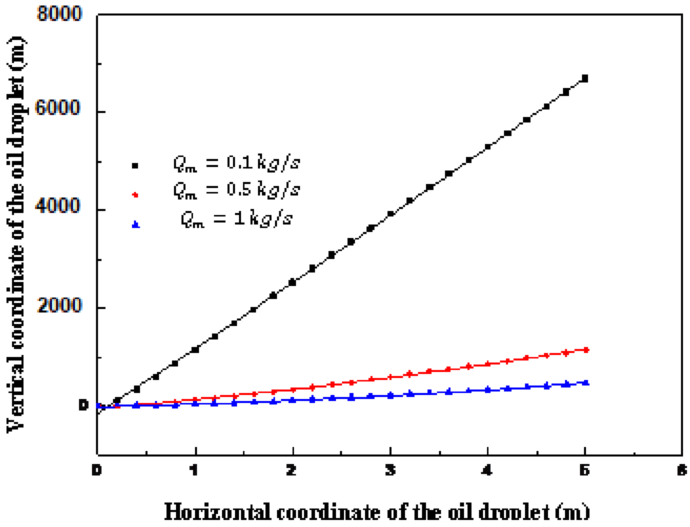


Figure 2. The influence of water mass flow rate on oil droplet trajectory in a horizontal flow regime

## 4. Results and discussions

### 4.1 Effect of influent water flow rate on droplet trajectory

The mass flow rate of wastewater directly determines the horizontal velocity within the separator and therefore significantly influences droplet trajectory. Fig. 2 presents droplet trajectories for various mass flow rates, ranging from low to high values. At low flow rates (typically below 0.5 $kg/s$ in this study), buoyancy forces dominate, allowing droplets to rise vertically with minimal horizontal displacement. Under these conditions, Archimedes' thrust remains the primary force governing droplet motion, ensuring efficient separation.

As the flow rate increases beyond this threshold, the horizontal drag force becomes increasingly significant. The droplet trajectory becomes elongated, with vertical ascent delayed by the stronger horizontal flow. At excessively high flow rates, horizontal motion dominates, potentially carrying droplets toward the outlet before they can reach the oil collection layer. The pronounced deformation of the trajectories at higher flow rates also suggests that inertial effects become more important, indicating that the laminar flow assumption may approach its limit of validity under these operating conditions. Operating beyond this threshold may require additional analysis accounting for transitional or turbulent flow effects.

### 4.2 Effect of initial velocity

The initial velocity of wastewater entering the separator is a critical hydrodynamic parameter governing droplet trajectory. To quantify its effect, Fig. 3 shows the vertical displacement $y$ versus horizontal distance $x$ for inlet velocities varying from 0.1 $to$ 0.5 $cm/s$. The trajectories are linear, indicating a constant ratio between vertical rise velocity and horizontal advection. As the inlet velocity increases, the slope of the trajectory increases significantly. This reflects the stronger horizontal transport of the droplet along the separator. At higher velocities, the droplet travels a

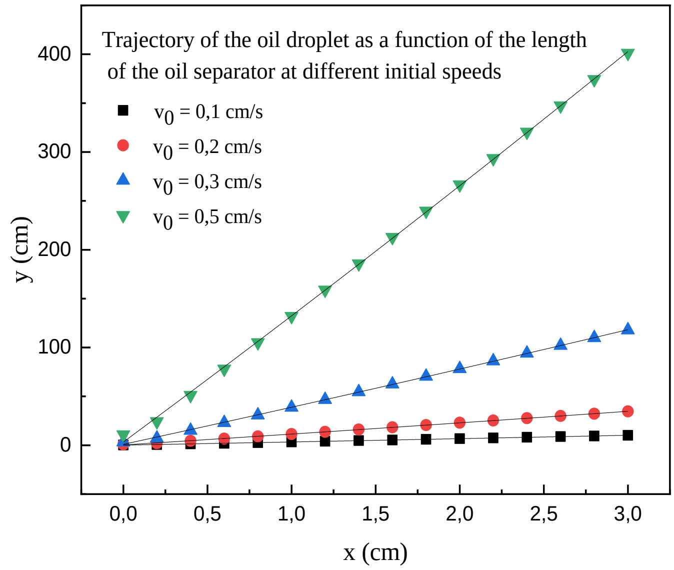


Figure 3. Oil droplet trajectories according to different initial velocities

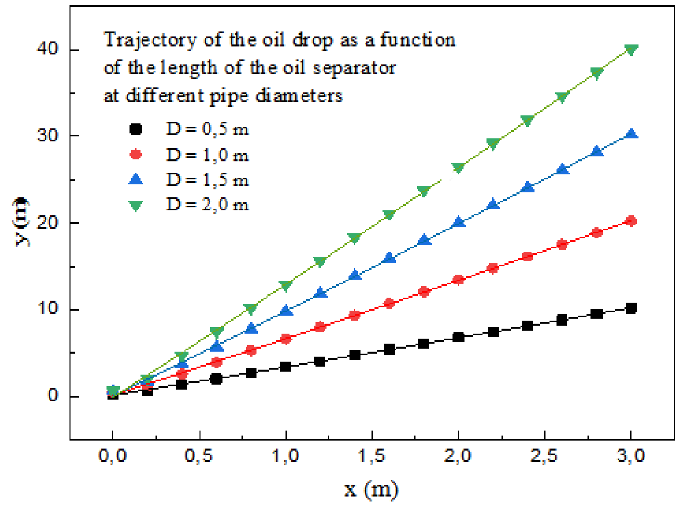


Figure 4. Droplet trajectories for different separator diameters

greater horizontal distance for the same vertical rise, implying that a longer separator is required to achieve complete flotation.

### 4.3 Effect of separator diameter

The internal diameter of the separation compartment is a fundamental geometric parameter that directly influences flow velocity and, consequently, droplet trajectory. To quantify this effect, droplet trajectories were computed for four different separator diameters ($D$ = 0.5, 1, 1.5 and 2.0

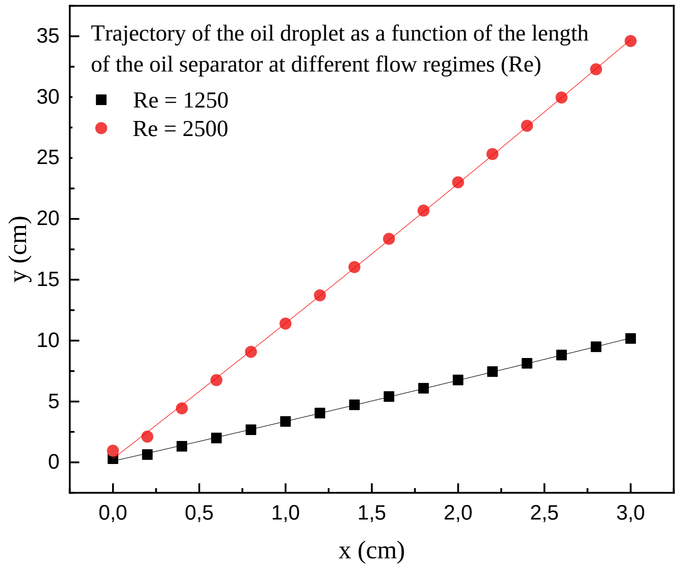


Figure 5. Comparison of droplet trajectories for laminar and transitional flow regimes

m) under constant mass flow rate conditions. Fig. 4 presents these trajectories, illustrating how diameter governs the path of oil droplets and the required separator length for complete oil recovery.

For a given mass flow rate, the horizontal velocity is inversely proportional to the cross-sectional area ($v_x = Q_m/S = 4Q_m/(\pi D^2)$). Larger diameters therefore reduce horizontal velocity, allowing droplets more time to rise vertically under buoyancy.

### 4.4 Effect of flow regime

To assess the impact of flow regime on separation performance, droplet trajectories were computed for two distinct Reynolds numbers. Fig. 5 compares the vertical displacement $y$ of an oil droplet as a function of separator length $x$ for $Re = 1250$ (laminar) and $Re = 2500$ (transitional/ turbulent). This comparison illustrates how the transition from laminar to turbulent flow alters droplet ascent, directly influencing separator efficiency.

A clear increase in slope is observed at higher Reynolds number. This indicates that as inertial forces become more significant relative to viscous forces, horizontal transport intensifies. The droplet is carried further downstream before reaching a given vertical position.

The results demonstrate that even within the laminar regime, increasing Reynolds number alters the balance between buoyancy-driven rise and convective transport. Higher $Re$ values therefore require greater separator length to maintain effective separation.

### 4.5 Combined effect of flow regime and separator scale on droplet ascent

While Reynolds number alone defines flow regime, its normalization by separator diameter ($Re/D$) accounts for geometric scaling effects. Fig. 6 illustrates droplet vertical displacement as a function of $Re/D$ across the laminar range ($Re = 100–2000$), demonstrating how this combined

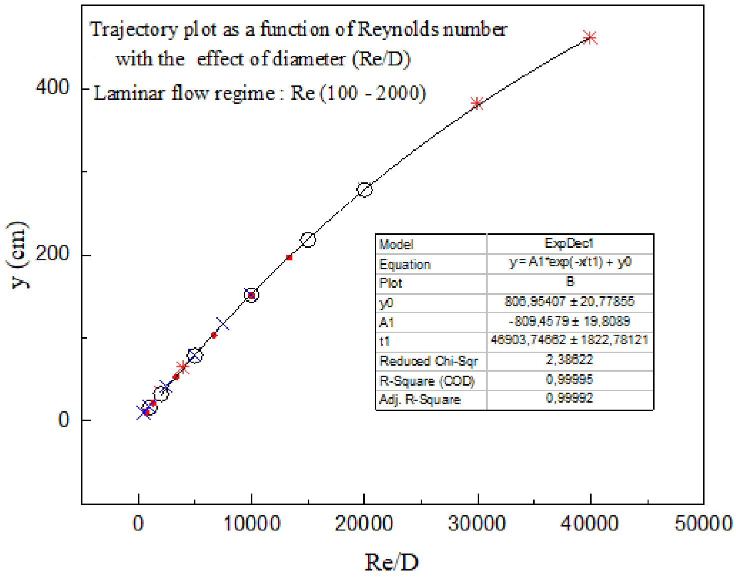


Figure 6. Influence of the $Re/D$ ratio on droplet vertical displacement under laminar regime ($Re = 100–2000$)

parameter can guide the selection of appropriate separator dimensions for a given flow condition. A strong nonlinear relationship is observed between droplet vertical displacement and the normalized parameter $Re/D$, following a clear exponential-type trend. This confirms that trajectory behavior can be reliably described through hydrodynamic scaling using $Re/D$.

The result highlights that separation dynamics are governed not only by Reynolds number but also by geometric scaling through diameter. The normalization by diameter emphasizes the coupling between hydrodynamics and separator geometry, demonstrating that droplet trajectory is highly sensitive to combined flow–geometry effects.

### 4.6 Estimation of the theoretical maximum length of the oil separator

The length of an oil separator (hydrocarbon separator) is calculated based on the peak flow rate and the rise velocity of oil particles, often designed to ensure sufficient residence time. Typical dimensions for standard installations range from 2 to over 10 meters in length, often exceeding 6 meters for settling/oil separation tanks. The sizing of the oil separator depends on the flow rate: the higher the flow rate, the longer the structure must be to ensure separation. Thus, the rise velocity depends on the size of the oil particles to be separated.

In summary, for a standard installation, the length often exceeds the width, with a typical length of several meters for flow rates on the order of tens of liters per second, ensuring effective separation before discharge. The derivative of the trajectory equation ($y$) with respect to the horizontal distance of the separator ($x$), based on Eq. (6), is:

$$\frac{dy}{dx} = \frac{b}{av_0}\left(1 - e^{-\frac{a}{v_0}x}\right) \tag{13}$$

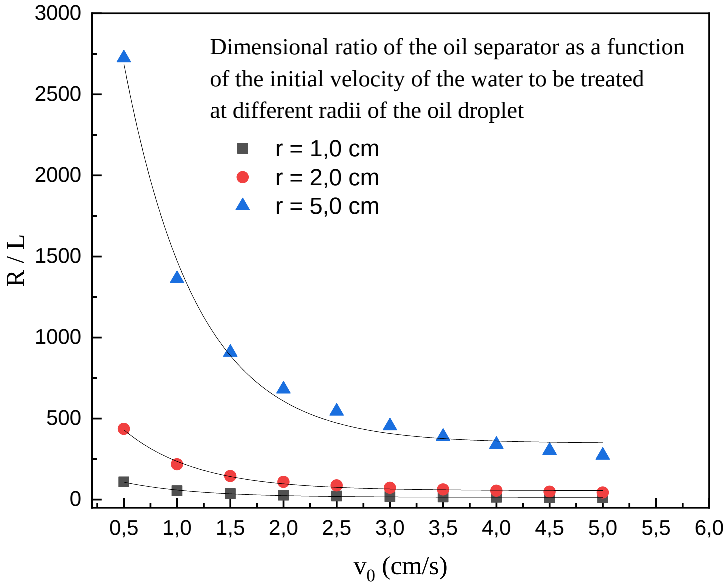


Figure 7. Effect of inlet velocity and droplet radius on the dimensional separation ratio (R/L)

At the separator inlet ($x = 0$), the slope is zero, indicating horizontal entry. As $x$ increases, the slope asymptotically approaches a maximum finite value $b/(av_0)$. For a separator of sufficient length, this asymptotic slope can be used as an approximation. Integrating under this approximation gives the relationship between separator radius $R$ and length $L$: $R/L = b/(av_0)$.

Substituting the expressions for $a$ and $b$ yields:

$$\frac{R}{L} = \frac{2}{9}\frac{r^2 g}{\mu v_0}\left(\frac{\rho_w}{\rho_{oil}} - 1\right) \tag{14}$$

This expression relates the separator geometry to the oil droplet properties, water viscosity, and inlet velocity.

Fig. 7 illustrates the variation of the dimensional separation ratio $R/L$ as a function of the initial water velocity $v_0$ for droplet radii of $100, 200, and\ 500\ \mu m$. For all droplet sizes, $R/L$ decreases nonlinearly with increasing inlet velocity, exhibiting a sharp decline at low velocities followed by a gradual asymptotic stabilization at higher velocities. This behavior indicates that higher inflow velocities necessitate a longer separator to provide adequate residence time for droplets to rise.

Moreover, the separation ratio increases significantly with droplet radius at any given velocity, demonstrating the strong impact of droplet size on separator design parameters. The droplet radius exerts a strong influence on the separation ratio due to its quadratic effect on the buoyancy-driven rise velocity (or terminal rise velocity $u_t$) under laminar conditions ($u_t \propto r^2$). As a result, the balance between horizontal advection and vertical migration scales approximately with $v_0/r^2$, making the system highly sensitive to droplet size. The separation between the curves demonstrates that larger droplets significantly alter the geometric separation requirement, particularly in the low-velocity regime where buoyancy and advection are comparable. Although the sensitivity decreases at higher velocities, droplet size remains a key governing parameter in separator design.

This study serves as a practical tool for preliminary sizing: for a target flow rate (which sets $v_0$) and known droplet size distribution, one can estimate the required $R/L$ and hence the separator length once the separator radius $R$ is chosen.

For a credible industrial design, the key is to select a flow rate that results in a balanced proportion between length and radius, typically within a length-to-diameter ratio of $3:1$ $to$ $5:1$, to ensure both hydraulic efficiency and practical geometry. To ensure robust performance in a real application, the theoretical length derived from this model is often multiplied by a safety factor (typically $1.5$ $to$ $3$) to achieve the effective ratio $(3:1-5:1)$. This practice balances the dimensions, preventing hydraulically inefficient units and ensuring effective oil-water separation.

## 5. Conclusions

This study developed a hydrodynamic trajectory model for horizontal oil-water separators, based on fundamental force balance and parametric analysis. The trajectory of an oil droplet is governed by the competition between buoyancy and drag forces. For the smallest target droplet (typically $50$ $\mu m$), the terminal rise velocity is low, requiring sufficient residence time to reach the top of the separator before exiting. From the condition that residence time must equal or exceed rise time, a direct relationship between separator geometry and operating parameters is derived, Eq. (12). The required separator length increases linearly with inlet velocity and inversely with the square of droplet radius. This explains why smaller droplets and higher flow rates demand longer separators, and why maintaining low inlet velocities is essential for compact designs. For typical design conditions (inlet velocity of $0.005$ $m/s$ and separator radius of $1.0$ $m$), Eq. (12) yields a minimum length of approximately $4.5$ $m$ for separating $50$ $\mu m$ droplets, with a corresponding residence time of about $15$ $mn$, Eq. (11).

The analysis also identifies a critical flow rate below which buoyancy forces dominate and above which horizontal advection compromises separation efficiency. This threshold, together with the laminar flow criterion, defines the safe operating envelope for the separator. Exceeding these limits leads to elongated trajectories and potential droplet carry-over. For a separator diameter of $1.0$ $m$, Eq. (8) gives a maximum inlet velocity of $0.015$ $m/s$ for maintaining laminar conditions, and the corresponding critical mass flow rate is $0.5$ $kg/s$.

Larger droplets rise significantly faster, as shown by the terminal velocity expression in Eq. (8). For example, $200$ $\mu m$ droplets require less than $0.6$ $m$ of length under the same conditions according to Eq. (12), confirming that the smallest target droplet governs the design. A model based on this worst case ensures that all larger droplets are separated even more efficiently, highlighting the importance of characterizing influent droplet size distribution in practical applications.

The theoretical analysis yields a direct relationship between separator radius and length. For the design droplet and typical operating velocity, Eq. (14) produces a theoretical length-to-diameter ratio of approximately 2.3. To account for unmodeled phenomena such as coalescence time, flow non-idealities, and short-circuiting, a safety factor of $1.5$ $to$ $2.0$ is recommended, bringing the practical design into the range of $3.4$ $to$ $4.6$, which aligns with the $3:1$ $to$ $5:1$ ratio commonly cited for separator dimensions in industry standards.

Based on this analysis and the governing Eqs. (8-12, 14), the following design guidelines are established: the separator diameter should be sufficiently large (typically $\geq 1.0$ $m$) to maintain laminar flow at the design flow rate; inlet velocity must be limited to $0.015$ $m/s$ or less to ensure adequate residence time for the smallest target droplet; separator length is the product of inlet velocity and droplet rise time, with a safety factor applied for robust performance; and the separation compartment should occupy approximately one-third of the total separator volume, following standard practice.

This approach is particularly useful for applications where complex simulation tools are unavailable, offering a balance between theoretical rigor and practical applicability. Incorporating fully realistic representations of coalescence, droplet size distributions, and non-ideal flow patterns would require experimental validation and/or multiphase modeling approaches (e.g., population balance models or CFD-based interface tracking), which are beyond the scope of the current study. Future work may extend the model in these directions, further enhancing its predictive capability for specialized applications.

## References

1. Managi, S., Opaluch, J.J., Jin, D., Grigalunas, T.A. (2015). Environmental regulations and technological changes in the offshore oil and gas industry. Land Economics, 81(2), 303-319. https://doi.org/10.3368/le.81.2.303
2. Ashraf, M.A., Shafiq, U., Mukhtar, A., Saeed, M.M. (2015). Design of industrial gravity type separators for the hydrocarbons and heavy oil-water separations. Research Journal of Chemical Sciences, 5(9), 72-75.
3. Pintor, A.M.A., Vilar, V.J.P., Botelho, C.M.S., Boaventura, R.A.R. (2016). Oil and grease removal from wastewaters: Sorption treatment as an alternative to state-of-the-art technologies—A critical review. Chemical Engineering Journal, 297, 229-255. https://doi.org/10.1016/j.cej.2016.03.121
4. Rodríguez-Restrepo, Y.A., Orrego, C.E. (2020). Immobilization of enzymes and cells on lignocellulosic materials. Environmental Chemistry Letters, 18, 787-806. https://doi.org/10.1007/s10311-020-00988-w
5. Shui, G., Zhao, Q., Chu, H., Zhou, X., Zhang, Y. (2025). Engineering the surface wettability: Recent advances in oil-water separation membranes. Energy & Environmental Sustainability, 1(3), 100040. https://doi.org/10.1016/j.eesus.2025.100040
6. Chen, S.S., Sun, Y., Tsang, D.C.W., Graham, N.J.D., Ok, Y.S., Feng, Y., Li, X.D. (2017). Potential impact of flowback water from hydraulic fracturing on agricultural soil quality: Metal/metalloid bioaccessibility, Microtox bioassay, and enzyme activities. Science of The Total Environment, 579, 1419-1426. https://doi.org/10.1016/j.scitotenv.2016.11.141
7. Pinheiro, C.T., Quina, M.J., Gando-Ferreira, L.M. (2021). Management of waste lubricant oil in Europe: A circular economy approach. Critical Reviews in Environmental Science and Technology, 51(18), 2015-2050. https://doi.org/10.1080/10643389.2020.1771887
8. Zhong, C., Nesbø, C.L., von Gunten, K., Zhang, Y., Shao, X., Jin, R., ... Alessi, D.S. (2022). Complex impacts of hydraulic fracturing return fluids on soil microbial community respiration, structure and functional potentials. Environmental Microbiology, 24(9), 4108-4123. https://doi.org/10.1111/1462-2920.16009
9. Stewart, M., Arnold, K. (2011). Produced water treatment field manual. Gulf Professional Publishing.
10. Oshinowo, L.M., Choi, Y.C., Ahmed, E.A., Al Abdulgader, H.A. (2022). Separation processes for sustainable produced water treatment and management. In Sustainable Separation Engineering: Materials, Techniques and Process Development, 105-154. Wiley. https://doi.org/10.1002/9781119740117.ch3
11. Khosravi, A., Abdollahi, F., Abbasi, M., Hashemifard, S.A. (2023). Oil field produced water: Issues and possible solutions. In S. Joshi, P. Jadhawar, A. Kumar (Eds.), Challenges and Recent Advances in Sustainable Oil and Gas Recovery and Transportation, 259-282. Gulf Professional Publishing. https://doi.org/10.1016/B978-0-323-99304-3.00014-5

12. Zhang, H., Li, K., Liu, T., Liu, Y., Hu, J., Zuo, Q., Jiang, L. (2025). Analysis of radial hydraulic forces in centrifugal pump operation via Hierarchical Clustering (HC) algorithms. Applied Sciences, 15(18), 10251. https://doi.org/10.3390/app151810251
13. Kato, S., Kansha, Y. (2024). Comprehensive review of industrial wastewater treatment techniques. Environmental Science and Pollution Research, 31(39), 51064-51097. https://doi.org/10.1007/s11356-024-34584-0
14. Khaleel, M.R., Ahsan, A., Imteaz, M., El-Sergany, M.M., Nik Daud, N.N., Mohamed, T.A., Ibrahim, B.A. (2015). Performance of GACC and GACP to treat institutional wastewater: A sustainable technique. Membrane Water Treatment, 6(4), 339-349. https://doi.org/10.12989/mwt.2015.6.4.339
15. Ahuja, M., Verma, V., Kaul, M., Kumar, L., Kumar, S. (2024). Biological wastewater treatment. In S. Pandit, L. Kumar, A.S. Mathuriya, D.A. Jadhav, S. Ray (Eds.), Advancements in Bio-systems and Technologies for Wastewater Treatment, 1-15. Springer. https://doi.org/10.1007/978-3-031-58331-5_1
16. Sravan, J.S., Matsakas, L., Sarkar, O. (2024). Advances in biological wastewater treatment processes: Focus on low-carbon energy and resource recovery in biorefinery context. Bioengineering, 11(3), 281. https://doi.org/10.3390/bioengineering1103281
17. Jayaraman, J., Kumaraswamy, J., Rao, Y.K.S.S., Karthick, M., Baskar, S., Anish, M., ... Ammarullah, M.I. (2024). Wastewater treatment by algae-based membrane bioreactors: A review of the arrangement of a membrane reactor, physico-chemical properties, advantages and challenges. RSC Advances, 14(49), 34769-34790. https://doi.org/10.1039/D4RA04417G
18. Ren, K., Miao, J., Qing, H., Xu, W., Zhang, X., He, Z., ... Lu, F. (2025). Probing to dynamics of a tube-core sandwich enhanced liquid-filled tank subjected to hydrodynamic ram. Thin-Walled Structures, 215, 113573. https://doi.org/10.1016/j.tws.2025.113573
19. Yang, X., Puig, V., Wang, X., Wang, S., Sun, C., Zhang, Y. (2025). Dynamic-high-gain-based decentralized optimal fault-tolerant control for a class of interconnected nonlinear systems. IEEE Transactions on Automatic Control, 70(9), 5823-5835. https://doi.org/10.1109/TAC.2025.3546545
20. Bellil, M., Dahmani, S., Bellil, A. (2026). Hydrodynamic modeling and dimensioning of an oil-water separator with automated control. Membrane and Water Treatment, 17(1), 83-101. https://doi.org/10.12989/mwt.2026.17.1.083

## Nomenclature

Roman Symbols

| Symbol | Definition | Unit |
|---|---|---|
| $A, B, C$ | Coefficients in the final droplet trajectory equation | $1, m, m^{-1}$ |
| $C_1$ | Conductivity sensor | - |
| $a, b$ | Coefficients in the simplified differential equation | $s^{-1}, m.s^{-2}$ |
| $d$ | Diameter (typically of inlet pipe or separator) | $m$ |
| $F_{ar}$ | Archimedes' thrust (buoyancy force) | $N$ |
| $F_x$ | Thrust force created by the water flow | $N$ |
| $F_y$ | Upward force (Vertical) | $N$ |
| $\mathrm{f_r}$ | Friction force | $N$ |
| $g$ | Gravitational acceleration | $m.s^{-2}$ |
| $L$ | Length of separator | $m$ |
| $P$ | Weight of the oil droplet | $N$ |
| $Q_m$ | Mass flow rate | $kg.s^{-1}$ |
| $R$ | Radius of the inlet separator | $m$ |

| | | |
|---|---|---|
| $R_e$ | Reynolds number | - |
| $r$ | Radius of the oil droplet | $m$ |
| $S$ | Cross-sectional area | m$^2$ |
| $t$ | Time | $s$ |
| $u$ | Rise velocity | $m.s^{-1}$ |
| $V_{1,2,3}$ | Solenoid valves | - |
| $V_{oil}$ | Volume of the oil droplet | $m^3$ |
| $v$ | Velocity | $m.s^{-1}$ |
| $v_0$ | Inlet velocity | $m.s^{-1}$ |
| $x, y$ | Horizontal and vertical displacements | $m$ |

Greek Symbols

| Symbol | Definition | Unit |
|---|---|---|
| η | Dynamic viscosity | $Pa.s$<br>$kg.m^{-1}.s^{-1}$<br>$N.s.m^{-2}$ |
| μ | Kinematic viscosity | m.s$^{-2}$ |
| $\rho$ | Density | $Kg.m^{-3}$ |

Subscripts

| res | Residence (for time) |
|---|---|
| t | Terminal |
| $w$ | Water |
| res | Residence (for time) |

## Appendix: Quantitative design parameters derived from trajectory analysis:

Summary of key numerical parameters derived from this study:

| Parameter | Symbol | Value | Units | Condition/Source |
|---|---|---|---|---|
| Droplet radius (smallest target) | $r_{min}$ | 50 | $\mu m$ | / |
| Oil density | $\rho_{oil}$ | 900 | $kg/m^3$ | Typical light hydrocarbons |
| Water density | $\rho_w$ | 1000 | $kg/m^3$ | At $20^o C$ |
| Dynamic viscosity of water | $\eta_w$ | 0.001 | $Pa.s$ | / |
| Terminal rise velocity | $u_t$ | 0.0087 | m/s | For $r = 200\mu m$, $R = 1m$ $and\ v_0 = 0.005 m/s$ |
| Rise time | $t_{rise}$ | 115 | s | // |
| Residence time | $t_{res}$ | 400 | s | // and $L = 2m$ |
| Minimum separator length | $L_{min}$ | 0.58 | m | Complete separation condition $t_{res} \geq t_{rise}$ |
| Inlet velocity | $v_0$ | 0.005 | m/s | Typical value for laminar flow regime |

| | | | | |
|---|---|---|---|---|
| Droplet Reynolds number | $Re_d$ | 0.11 | – | Stokes valid where $r = 50\mu m$ |
| Critical flow Reynolds number | Re | 2300 | – | Laminar if Re < 2300 |
| Critical mass flow rate | $Q_m$ | 0.5 | kg/s | For $D = 1m$ $and\ v_0 = 0.005\ m/s$ |
| Length/Diameter ratio | $L/D$ | 3.4 to 4.6 | – | For $r = 50\mu m$ with safety factor SF = 1.5-2.0 |
| Parameter | Symbol | Value | Units | Condition/Source |